



RISK-BASED EVALUATION OF LANDFILL GAS FLARE EFFICIENCY Using Computational Fluid Dynamics (CFD)

Dr. Rouzbeh Abbassi and Professor Kelly Hawboldt, Process Engineering Department
Faculty of Engineering and Applied Science, Memorial University of Newfoundland
April 2012



This research project was funded under the The Harris Centre – MMSB Waste Management Applied Research Fund. The intellectual property vests with the author(s). For more information about this Research Fund to obtain hard copies of this report, please contact the Harris Centre.

Final Report

Risk-based Evaluation of Landfill Gas Flare Efficiency Using Computational Fluid Dynamics (CFD)

Dr. Rouzbeh Abbassi and Professor Kelly Hawboldt

Process Engineering Department, Faculty of Engineering and Applied Science,

Memorial University of Newfoundland

St. John's, NL, Canada

Waste Management Applied Research Fund 2010-2011

Harris Centre

Memorial University

April 20th, 2012

Abstract

Methane is produced in landfills through the anaerobic digestion of organic material. Methane is a greenhouse gas with 24.5 times the global warming potential when compared to carbon dioxide (CO₂). Landfill gas also contains hydrogen sulfide which may account for up to 1 percent by volume of landfill gas emissions and impacts human health even in low concentrations. As a result, landfill gas is typically collected and either flared (to convert methane and hydrogen sulphide to carbon dioxide and sulfur dioxide respectively) or used for power on site. Flaring is typically an incomplete combustion process, producing many other pollutants that may result in environmental and human health impacts. Quantifying these emissions would result in better flare designs and plume dispersion estimates. However, the efficiency of flare combustion is site and flare design specific, making predictions difficult. In this work a Computational Fluid Dynamics (CFDs) model (using Fluent as a tool) was developed to simulate the flow and combustion mechanisms of the flare. The model can be used as a tool in flare design and as a method to ensure an operating flare is working properly. It can also be used to predict dispersed gases concentrations, allowing operators to optimize environmental monitoring stations and flare operations. The model is a function of the input data and therefore critical parameters such as exit gas velocities, stack height and diameter among other parameters must be specified. The model was validated using lab data from published work. A risk assessment model is proposed as part of this work which integrates the CFD model with a risk model.

Keywords: Landfill gas, Flaring, Reaction mechanism, CFD, Environmental risk assessment

Abstract	2
Table of Contents	3
Chapter 1: Introduction	5
1.1. Introduction	5
1.2. Objectives	5
1.3. Scope	6
Chapter 2: Gas Composition	7
2.1. Landfill gas composition	7
2.2. Flare gas composition	10
Chapter 3: CFD Modeling	12
3.1 Flare CFD modeling	12
3.1.1 Governing equations	12
3.1.1.1 Mass and species transport	13
3.1.1.2 Momentum transport	13
3.1.1.3 Energy transport	13
3.2 Flared studies: A case study	14
3.2.1 Chemistry	14
3.2.2 Modeling parameters	14
3.3 Results and discussion	15
Chapter 4: Environmental Risk Assessment	18
4.1 Environmental risk assessment	18
4.1.1 Hazard identification and assessment	23
4.1.2 Exposure assessment	24
4.1.3 Dose-response assessment	29
4.1.4 Risk characterization	31
4.2 A developed risk-based methodology	32
4.3 A risk-based methodology: A case study	33

4.3.1	Specification of a considered site	34
4.3.2	Risk analysis	34
Chapter 5: Conclusion		36
5.1	Conclusion	36
5.2	Recommendation for future works	36
Acknowledgment		36
References		37
Appendix 1		40
Appendix 2		42

1.1. Introduction

The atmospheric methane burden has more than doubled and the tropospheric methane concentration has increased at an approximate rate of 1% per year over the past two centuries. Landfill gas is typically 40%-60% methane which has 24.5 times the global warming potential of carbon dioxide (CO₂) over a hundred year period. Hydrogen sulfide can make up to 1% by volume of landfill gas and impacts human health even in low concentration of 30 ppb (Alian, 1997). In addition landfill gas has been found to contain as many as 550 trace components (EPA, 2002). As a result, collection and flaring of the landfill gas has been used to decrease the intensity of the Green House Gas (GHG) emissions and convert toxic gases to more benign compounds (e.g. H₂S to SO₂). In the past it was assumed the flare achieved 98% combustion efficiency (EPA, 2002). However, studies by the Alberta Research Council and others have shown that flare combustion efficiency can be as low as 64% depending on flare feed gas composition, wind speeds, and other factors. The control of flare combustion is limited due to lack of control over air/fuel ratios, temperature, and combustion time. As a result of incomplete combustion products are formed which can be more toxic than the landfill gas compounds. Landfill gas is utilized to generate waste based power and/or heating, however the low levels of methane limit this use. Further inerts such as nitrogen and water vapor decrease the heating value of the gas and other compounds such as H₂S are corrosive and toxic, limiting use as a fuel. The gas must typically be treated to meet boiler/engine standards. As such, the traditional method of disposing of landfill gas is flaring. As outlined above the lack of understanding of the combustion process within the flare and costs associated with field testing of flares complicate the management of flaring. In order to assess the risks associated with flared gas we must first have a reliable method to at the very least give good estimates of flare emissions. Once this is accomplished a risk-based approach can be used as a key to evaluate the impact and optimize the operation of the flare.

1.2. Objectives

The overall objective of this project is to further develop best management practices of landfill gas. We plan to combine a CFD model with a kinetic model to better predict flared gas compositions. Knowledge of the composition of the flared gas under different flaring scenarios would allow the operator to optimize flaring process parameters and management to maximize combustion and minimize the formation of toxic and/or undesirable contaminants.

Specific objectives include the following:

1. Identify range of possible feed gases (generated in landfill operations)

2. Develop a model to simulate flaring of gas and validate the model
3. Develop a methodology to determine impact of flaring based on modeling results, and propose alternative uses

1.3. Scope

The methodologies applied to this research are as follows:

1. Literature review of various types and composition of landfill gas and flare process parameters
2. CFD modeling of the landfill gas flare by application of Fluent (as a CFD tool) and considering different parameters which affect the combustion efficiency
3. Develop a risk-based methodology to evaluate the flare efficiency based on the landfill gas composition and ambient conditions

Chapter 2 Gas Composition

2.1. Landfill gas composition

Landfill gas is produced by the biological decomposition of wastes placed in a landfill (NRCAN, 2011). There is a significant variability in landfill gas composition based on the waste in the landfill. The gas is complex as outlined in Table 2.1.

Table 2.1. Average landfill gas composition (Eklund et al., 1998)

Average landfill gas composition (ppmv)			
Compound	Concn (ppmv)	Compound	Concn (ppmv)
Methane	55.63%	o-ethyltoluene	3.43
Carbon dioxide	37.14%	p-diethylbenzene	2.67
Oxygen	0.99%	m-ethyltoluene	2.49
Total NMOC	438.09	t-2-pentene	2.37
Ethane	222.61	o-xylene	2.17
Total unidentified VOCs	134.55	o-dichlorobenzene	2.17
Limonene	35.38	n-propylbenzene	2.09
Toluene	14.57	Styrene	2.02
n-decane and p-dichlorobenzene	13.97	1-undecene	2.02
p-isopropyltoluene	13.14	p-ethyltoluene	2.01
Propane	13.03	1,2,3-trimethylbenzene	1.90
Isobutane	8.24	Benzyl chloride and m-dichlorobenzene	1.88
a-pinene	7.85	1,3,5-trimethylbenzene	1.76
3-methylpentane	7.75	n-butylbenzene	1.50
Acetone	6.09	m-diethylbenzene	1.46
p-xylene+m-xylene	5.97	Dichlorodifluoromethane	1.27
n-undecane	5.50	Chlorobenzene	1.15
1,2,4-trimethylbenzene and t-butylbenzene	5.06	dichlorotoluene	1.15
Ethylbenzene	4.71	n-octane	0.99
1,3-butadiene	3.98	n-pentane	0.97
n-butane	3.80	Benzene	0.93
Isopentane	3.76	n-hexane	0.92
n-nonane	3.57	Isobutene + 1-butene	0.92

Brosseau and Heitz (1994) outline the major compounds in Table 2.2.

Table 2.2. Landfill gas composition (Brosseau and Heitz at 1994)

Compounds	Palos Verdes CA	C.T.E.D. Montreal QC
	% Vol	% Vol
Methane	53.283	60
Carbon Dioxide	45.588	37
Hydrogen	0.056	-
Oxygen	0.070	0.1
Nitrogen	0.272	2.8
Trace Gases	0.731	0.1

Kim, 2006 outlined the impact of seasons and the age of the landfill on gas composition with respect to sulphur compounds (Table 2.3). This information is key in that some compounds will more readily combust than others and some are more toxic than others. Kim 2006 is not included in Refs.

Table 2.3. Reduced S compounds from each individual vent pipe (all units in ppb)

Season	Vent No.	H ₂ S	CH ₃ SH	DMS	CS ₂	DMDS
Spring	V1	2629	3400	1913	80.8	147
	V2	124,410	52.1	32.5	28.6	14.3
	V3	12,168	1387	397	76.3	18.2
	V4	11,463	1698	935	391	413
Summer	V1	6848	690	1011	163	313
	V2	523,838	253	347	302	146
	V3	192,013	1017	540	364	78.8
	V4	278,413	514	929	162	142
Fall	V1	437	5.88	30.2	3.12	9.36
	V2	200,431	53.3	13.7	27.0	4.32
	V3	280,970	97.1	65.4	20.6	2.96
	V4	108,234	30.8	26.5	48.0	3.48
Winter	V1	---	7.43	76.5	14.3	14.8
	V2	181,337	18.6	0.01	4.22	3.72
	V3	92,426	7.22	0.01	3.41	0.01
	V4	70,280	6.02	3.47	8.54	1.78

The seasonal variation of Volatile Organic Carbon (VOC) at the landfill in the city of Izmir, Turkey was studied by Dincer et al., in 2006. This investigation demonstrated that VOC concentrations were relatively low in September compared to May. ATSDR (2011) assessment of the composition of major compounds and their impact is summarized in Table 2.4.

Table 2.4. Typical landfill gas composition ATSDR (2011)

Component	Percent by volume	Characteristics
Methane	45-60	Methane is naturally occurring gas. It is colorless and odorless. Landfills are single largest source of U.S. man-made methane emissions
Carbon dioxide	40-60	Carbon dioxide is naturally found at small concentrations in the atmosphere (0.03%). It is colorless, odorless, and slightly acidic.
Nitrogen	2-5	Nitrogen comprises approximately 79% of the atmosphere. It is odorless, tasteless, and colorless.
Oxygen	0.1-1	Oxygen comprises approximately 21% of the atmosphere. It is odorless, tasteless, and colorless.
Ammonia	0.1-1	Ammonia is a colorless gas with a pungent odor.
NMOCs (non-methane organic compounds)	0.01-0.6	NMOCs are organic compounds (i.e., compounds that contain carbon). (Methane is organic compounds but is not considered as NMOC). NMOCs may occur naturally or be formed in synthetic chemical processes. NMOCs most commonly found in landfills include acrylonitrile, benzene, 1,1-dichloroethane, 1,2 -cis dichloroethylene, dichloromethane, carbonyl sulfide, ethylbenzene, hexane, methyl ethyl ketone, tetrachloroethylene, toluene, trichloroethylene, vinyl chloride, and xylenes.
Sulfides	0-1	Sulfides ((e.g. hydrogen sulfide, dimethyl sulfide, mercaptans) are naturally occurring gases that give the landfill gas mixture its rotten-egg smell. sulfides can cause unpleasant odors even at very low concentrations.
Hydrogen	0-0.2	Hydrogen is an odourless, colorless gas.
Carbon monoxide	0-0.2	Carbon monoxide is an odorless, colorless gas.

The composition is also a function of bacterial activity. The production phases of landfill gas can be seen in Figure 1. In addition to waste composition and age of refuse, the presence of oxygen in the landfill, moisture content and temperature affect the landfill gas composition.

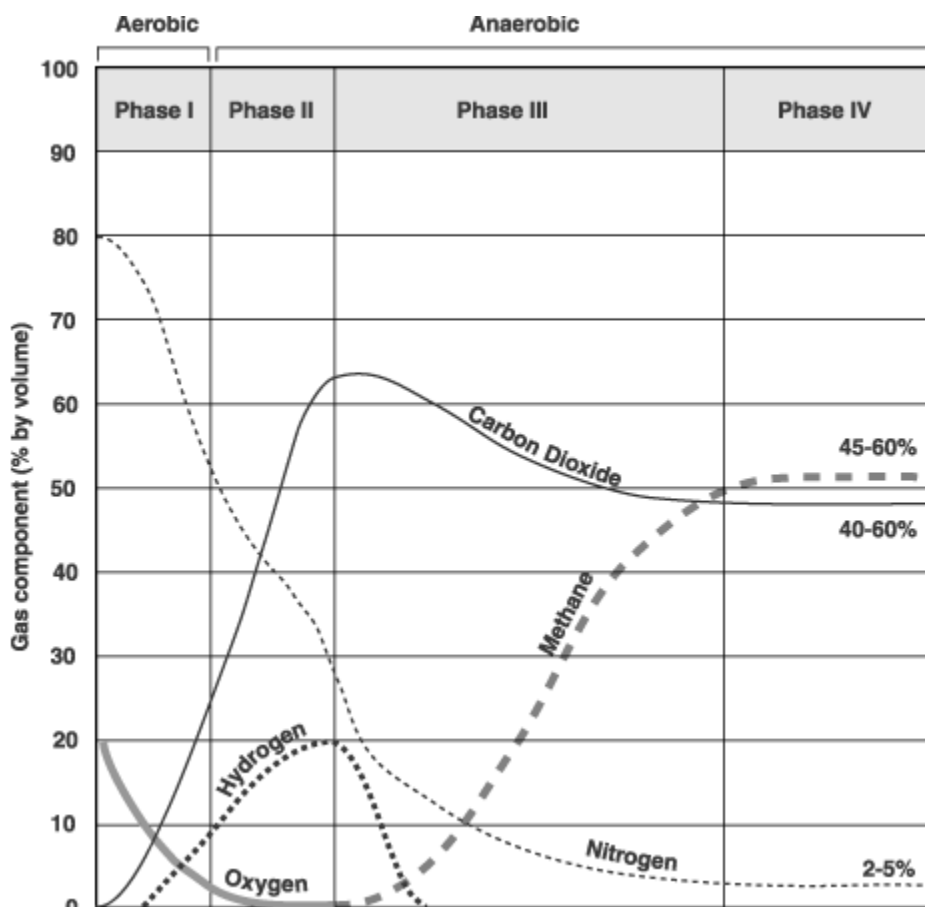


Figure 2.1. Production phases of typical landfill gas

2.2 Flare Gas Composition

The composition of incinerators, and other stacks associated with combustion products is very complex. Flares exhibit additional complexity due to the “open” or “diffusion” flame, where there is no control over the amount of fuel/air, mixing, and combustion time. The pollutants formed are a function of gas composition, flare design, and meteorological conditions. As a result, most regions use “common” pollutants to assess the impact of a gaseous emission on the environment.

The actual number of contaminants released in measureable amounts from a flare is significant. There have been limited studies of the composition of flares from refineries and gas plants. One of the most comprehensive was performed at ARC ((Stroscher, 1996)) where various natural and solution gas compositions were flared in a lab, at pilot scale, and at field scale. In the pilot scale experiment, of the 188 hydrocarbons detected in the emitted plume, many were polycyclic aromatic hydrocarbons (PAHs) which are major constituents of particulate matter. Further, in lab through to field studies, the presence of liquid hydrocarbons decreased CE by 10-12%. The field studies were of particular interest as sour associated gas from a well battery was tested. The inlet composition to the flare is outlined in Table 2.5.

Table 2.5. Sour Associated Gas Composition (Stroscher, 1996)

Compound	Mole %
Methane	45.4
Ethane	10.7
Propane	5.7
Butanes	2.4
Pentanes	2.6
Hydrogen Sulphide	22.8

There are significant gaps in the nature and emission rate of flared gas, however research is ongoing. The uncertainty results in difficulty in predicting downwind concentrations of pollutants. This uncertainty increases when coupled with the fact that most commercially available dispersion models are designed for continuous sources (such as compressor stacks or incinerators) rather than intermittent sources such as flares.

3.1. Flare CFD modeling

Different mathematical models based on the numerical solution of the fluid dynamics equations have been proposed for simulation and control of industrial combustion; however there is very little on flare modelling. The advantage to CFD simulation over physical prototypes is the ability to simulate the actual production platform rather than a smaller experimental model ((Ferguson, 2010)). Application of CFDs reduces the cost of using actual flare experiments, although the results received by CFDs are only as good as the input data. Further, inaccurate models lead to erroneous results. Castiñeira and Edgar, 2006a/b proposed the CFD tool Fluent for simulating two different types of flare. Three different combustion flames of different sizes and compositions were simulated and demonstrated close agreement between simulation and experimental data. The effect of crosswind on the combustion efficiency of the flames is also simulated by CFD (Castiñeira and Edgar, 2008a; 2008b; Gottimukkala, 2008). The results demonstrated that the high momentum flames are more sensitive to crosswinds whenever the jet velocity increases. The effect of cross wind velocity and exit jet is also investigated using CFD (Fluent) by Lawal et al., 2010. Results demonstrated that variation of these two parameters directly affect the flare efficiency. Using CFD models we are able to evaluate different variables such as cross wind velocity, flare tip diameter, heating value of the gas etc. on flare efficiency, temperature and gas composition profiles in the flame. The drawback to the published studies above is the lack of detail in the kinetic model, there was no study of emissions outside of carbon dioxide, and little detail on specifics such as pilot flame modelling etc... In this work, we first develop the CFD model, validate with published data (using a more complex kinetic model), and evaluate emissions outside of carbon dioxide. In our work a detailed reaction mechanism (containing 23 species and 74 reactions) was used.

3.1.1. Governing Equations

CFD is based on solving conservation or transport equations for mass, momentum, energy, and species. A set of partial differential equations consisting of six equations and six unknowns (density, three components of velocity, temperature and pressure) which are all the function of three spatial dimensions and time are given below:

3.1.1.1. Mass and species transport

Mass conservation can be expressed in terms of density or individual gaseous species (Y_α), as illustrated in equations 1 and 2 respectively.

$$\frac{\partial \rho}{\partial t} + \nabla \cdot \rho u = m_b''' \quad (3.1)$$

$$\frac{\partial}{\partial t} (\rho Y_\alpha) + \nabla \cdot \rho Y_\alpha u = \nabla \cdot \rho D_\alpha \nabla Y_\alpha + m_\alpha''' + m_{b,\alpha}''' \quad (3.2)$$

In equation 1, m_b''' is the production rate of the species by evaporating droplets or particles.

3.1.1.2. Momentum transport

$$\frac{\partial}{\partial t} (\rho u) + \nabla \cdot \rho u u + \nabla p = \rho g + f_b + \nabla \cdot \tau_{ij} \quad (3.3)$$

In equation 3, considering $u = [u, v, w]^T$, uu (dyadic tensor) is given by the tensor product of the vectors u and u^T , the term f_b is forces such as grad exerted from liquid droplets and τ_{ij} is stress tensor defined as follows:

$$\tau_{ij} = \mu (2S_{ij} - \frac{2}{3} \delta_{ij} (\nabla \cdot u)) \quad (3.4)$$

In equation 4, μ is the dynamic viscosity of the fluid and S_{ij} is the symmetric rate of strain tensor, defined as follows:

$$S_{ij} = \frac{1}{2} \left(\frac{\partial u_i}{\partial x_j} + \frac{\partial u_j}{\partial x_i} \right) \quad i, j = 1, 2, 3, \dots \quad (3.5)$$

This equation can be computed by a Direct Numerical Solution (DNS), wherein the dissipative terms are computed directly or Large Eddy Simulation (LES), wherein large scale eddies are computed directly and sub-grid scale dissipative processes are modeled.

3.1.1.3. Energy transport

$$\frac{\partial}{\partial t} (\rho h_s) + \nabla \cdot \rho h_s u = \frac{Dp}{Dt} + q''' q_b''' - \nabla \cdot q'' + \varepsilon \quad (3.6)$$

In this equation, the sensible enthalpy is the function of temperature, as follows:

$$h_s = \sum_\alpha Y_\alpha h_{s,\alpha} \quad \text{and} \quad h_{s,\alpha}(T) = \int_{T_0}^T C_{p,\alpha}(T') dT' \quad (3.7)$$

The term q_b''' in equation 6 is the heat release rate per unit volume from a chemical reaction, q_b''' is the energy transferred to the evaporating droplets, and q'' is conductive and radiative heat fluxes, calculated by equation 8, in which k is the thermal conductivity.

$$q'' = -k\nabla T - \sum_{\alpha} h_{s,\alpha} \rho D_{\alpha} \nabla Y_{\alpha} + q_b''' \quad (3.8)$$

3.2. Flared studies: A case study

To investigate the total emissions from the flared gases, a CFD model using Fluent integrated with detailed reaction mechanism has been developed. To validate a model, a case study of using an experimental flare (lab scale size) burning methane has been adopted from the literature. Ideally a landfill gas would be used as a case study. However, the published data regarding landfill flares do not include parameters such as flow rate and stack specifications. We visited the Robin Hood Bay facility to collect information on their flare operation. However, there was little data available. Further, the existing flare (a simple candle stick flare) is scheduled to be replaced by a larger scale industrial type flare. (At this time we will take the data from this flare and apply the methodology outlined below. Sentence unclear, which flare? The experimental flare (lab scale size) referred to above?

3.2.1. Chemistry

There have been great advances lately in obtaining detailed reaction mechanism that can describe hydrocarbon combustion in various temperatures and operating conditions (Mendiara et al., 2004). However, using a complex mechanism with hundreds of compounds increases computational cost (days to run models) with little gain in accuracy of predicting gas compositions and subsequent impact. A reduced mechanism accomplishes the goal of predicting combustion efficiencies accurately and predicting contaminants of concern in emissions. We first tested our CFD model with a very simple five global steps mechanism to ensure the model was running properly. We were able to predict CO₂ levels accurately, however, this mechanism was limited in the breadth of species involved (Peters and Kee, 1987; Bilger et al., 1990). We adopted the mechanism propped by Mendiara et al (2004) which has 23 species and 74 reactions.

3.2.2. Modeling parameters

We first needed to verify our CFD model and reaction mechanism. Castiñeira and Edgar studied a lab scale methane flare in 2008. In this study the diameter of the stack at the middle of the domain is 7.2 mm. The fuel contained 15% methane. To simulate open combustion, a two dimensional domain (0.7*0.7 m²) is used for this simulation. The model is defined and meshed in Gambit. Gambit is one of the well-

known and user-friendly preprocessor ((ANSYS, 2012) not in Refs) to create the geometry and meshing for importing to Fluent. (The overall 129,560 cells with the similar size considered in the domain. Sentence unclear). The primary temperature of the exit gas is considered at 2000 K. The temperature provides the ignition energy for the gases at the beginning. As most of the reactions in this mechanism are exothermic, the required extra heat for all the reactions in the flame will be supplied by the heat which is released from these reactions.

To model the combustion process with Fluent, the segregated, steady state solver is used for computations. The standard K- ϵ model that includes two extra transport equations to represent the turbulent properties of the flow is used without any change in default constant values of $C_{\epsilon 1}$ and $C_{\epsilon 2}$. The in situ adaptive tabulation (ISAT) method was used to save computational work that is a most powerful tool to accelerate detailed stiff chemistry. A speedup of two to three orders of magnitude (is assisted assists) a simulation that would take months without considering ISAT to be run in days instead ((Fluent, 2012)). The absolute and relative error tolerances were set as 1×10^{-6} and 1×10^{-9} , respectively. These values were previously used by Castiñeira, 2008 for a similar study. The ISAT error tolerance was set as 1×10^{-4} . The maximum storage capacity was set as 200 Mb. The reference time step was set as 0.001.

3.3. Results and discussion

After modeling the flare gas combustion by application of a methodology discussed in the previous sections, the results of CH₄ combustion and CO₂ production from the flared gases were compared with the experimental results. Figure 3.1. compares the experimental and simulation results of methane combustion in the middle axes of the flare. Both the data and the model show the same trend but at different distances in the flame. This is due to the fact that in the experiment the combustion process starts at some distance from the flare tip. However, in the simulated flare, as the gas and the air are exiting simultaneously from the flare tip with a high temperature, methane combustion occurs immediately after releasing from the tip. The critical aspect is that we were able to predict final product emissions, combustion efficiency, and temperature of the flame.

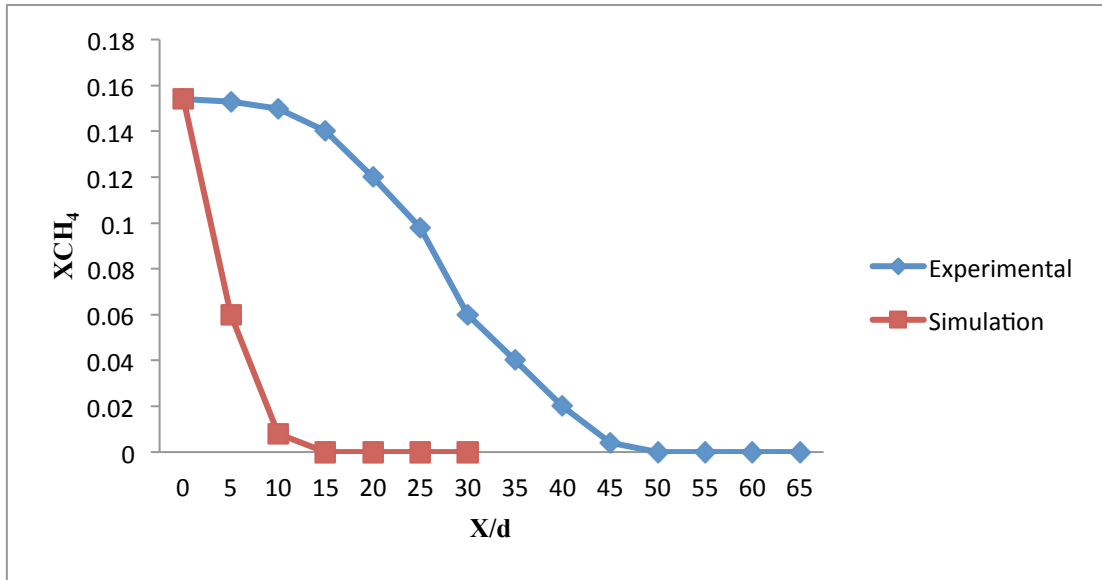


Figure 3.1. Experimental and simulation mass fraction of CH₄

The results of CO₂ mass fraction can be seen in Figure 3.2. The minimum mass fraction of CO₂ is 0.11 which is in agreement with the experimental results. However, the maximum in the simulation is achieved at a shorter distance from the flare tip. Again, this is a result of the reason stated above. Again the model matched both trend and concentrations in flame.

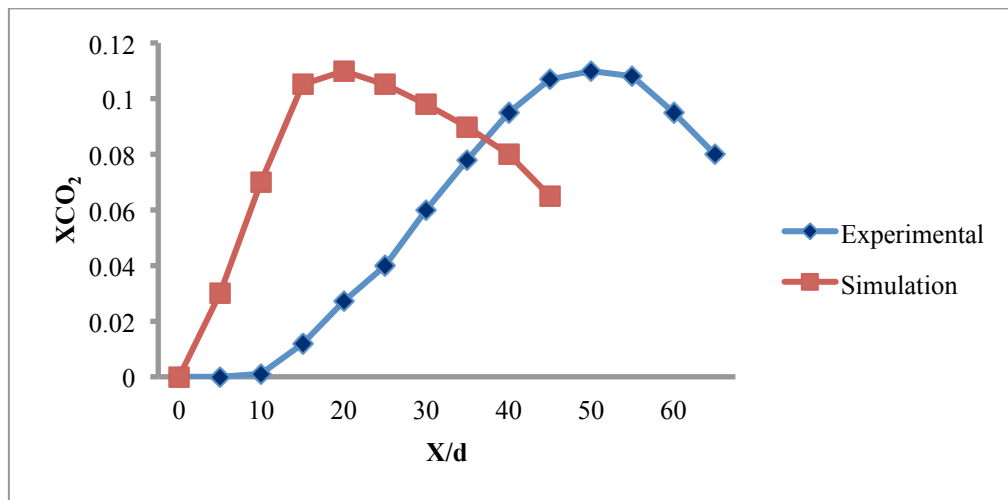


Figure 3.2. Experimental and simulation mass fraction of CO₂

After comparing the results of the methane combustion and CO₂ production from the simulation with experimental data, the concentration of other species existed in the considered reaction mechanism were also analyzed. We demonstrate this with the other major carbon species, carbon monoxide (CO), an important gas due to its toxicity and GHG effect. (Figure 3.3). The CO shows a peak early in the flame where we would expect the largest level of incomplete combustion products. There is no experimental data because the study did not consider other compounds. This demonstrates the use of the CFD model,

with the ability to predict compounds not measured due to lack of analytical or capture equipment on the flare.

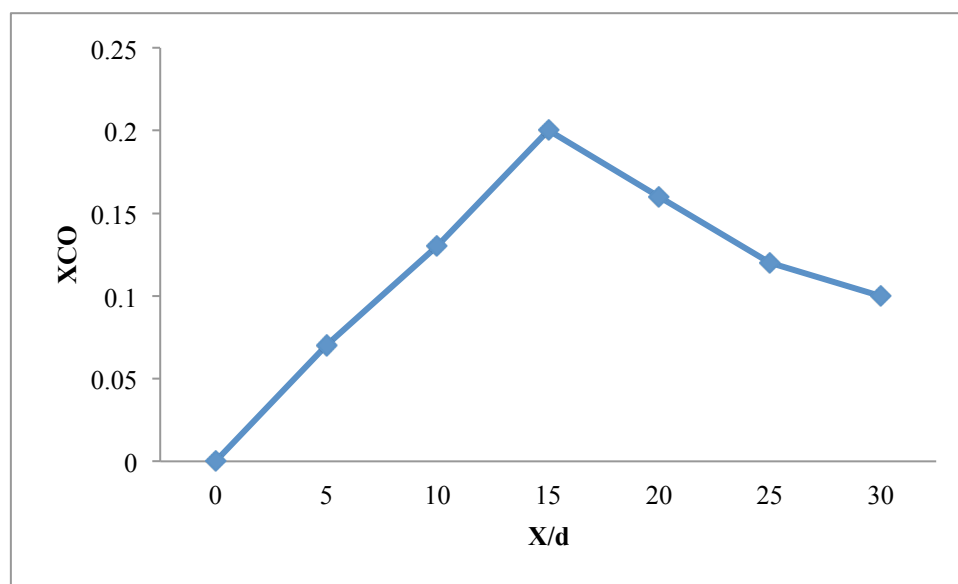


Figure 3.3. Simulation mass fraction of CO

As the experimental data from Castiñeira and Edgar (2008a) was in a controlled lab setting, the flare is able to achieve high combustion efficiencies. However, as (Stroscher (1996)) demonstrated, as one moves from a lab scale to pilot to field, and gas composition changes from pure methane to mixtures, the combustion efficiency drops. This is largely due to poor mixing between air and feed gas, where the air surrounds the flare rather than co-flowing with the fuel (as in the lab). The CFD model was adapted to account for this by tuning the air: fuel ratios to match emission of carbon dioxide. This is an example of how in an industrial flare, the CFD model must be combined with some basic emission data (this data is typically available as companies are to measure key components of the flare emissions). The CFD model can provide additional information about the nature of the emissions that would be extremely costly and technically difficult to obtain. Further, the model can determine combustion efficiency, effect of varying flow rates, stack height and diameter, and wind speed on emissions. We are continuing this work by using the developed model to predict actual landfill/industrial flares. Contaminants of concern in the gas emitted can be predicted as above and used to determine the impact of the flare on the surrounding area. From this type of analysis we can determine combustion efficiency, effect of varying flow rates, stack height and diameter, and wind speed on emissions. We are continuing this work by using the developed model to predict actual landfill/industrial flares. Our next step is to incorporate the mechanism outlined in Appendix 2 (with sulfur compounds) to predict emissions from flare gases containing H₂S.

4.1. Environmental risk assessment

Environmental risk analysis is a systematic process of assessing, managing and communicating risk to human health caused by an event or activity occurring in the environment. Risk analysis is a detailed examination that consists of risk assessment, risk evaluation and risk management alternatives that are produced to recognize the nature of unwanted, adverse consequences to human life, health, property and environment (Bondad et al., 2008). The Food and Drug Administration ((FDA, 2002) not in Refs) defines “risk analysis as a tool to enhance the scientific basis of regulatory decisions.” It includes risk assessment, risk management and risk communication activities. Each component has unique responsibilities. Risk assessment provides information on the extent and characteristics of the risk attributed to a hazard. Risk management includes the activities undertaken to control the hazard. Risk communication involves an exchange of information and opinion concerning risk and risk related factors between the risk assessors, risk managers and other interested parties (Fjeld et al. 2006). In simple terms:

$$\text{Risk analysis} = \text{risk assessment} + \text{risk management} + \text{risk communication}$$

These three components of risk analysis are dependent on one another for analyzing the magnitude of risk caused by the release of the contaminants, as can be seen in Figure 4.1. Environmental risk assessment is the characterization of adverse health effects that results from human and ecological exposures to environmental hazards. The field of environmental risk assessment has grown in the last two decades due to the increase in public concern about the adverse effect of chemicals and hazards to the wildlife and ecosystem. Environmental risk assessment uses a set of tools to identify the likelihood and magnitude of adverse effects posed by environmental agents on human health and to natural resources. Conclusively, risk assessment is a systematic process for describing and quantifying the risk related to hazardous substances, processes, actions, or events (Covello et al., 1993).

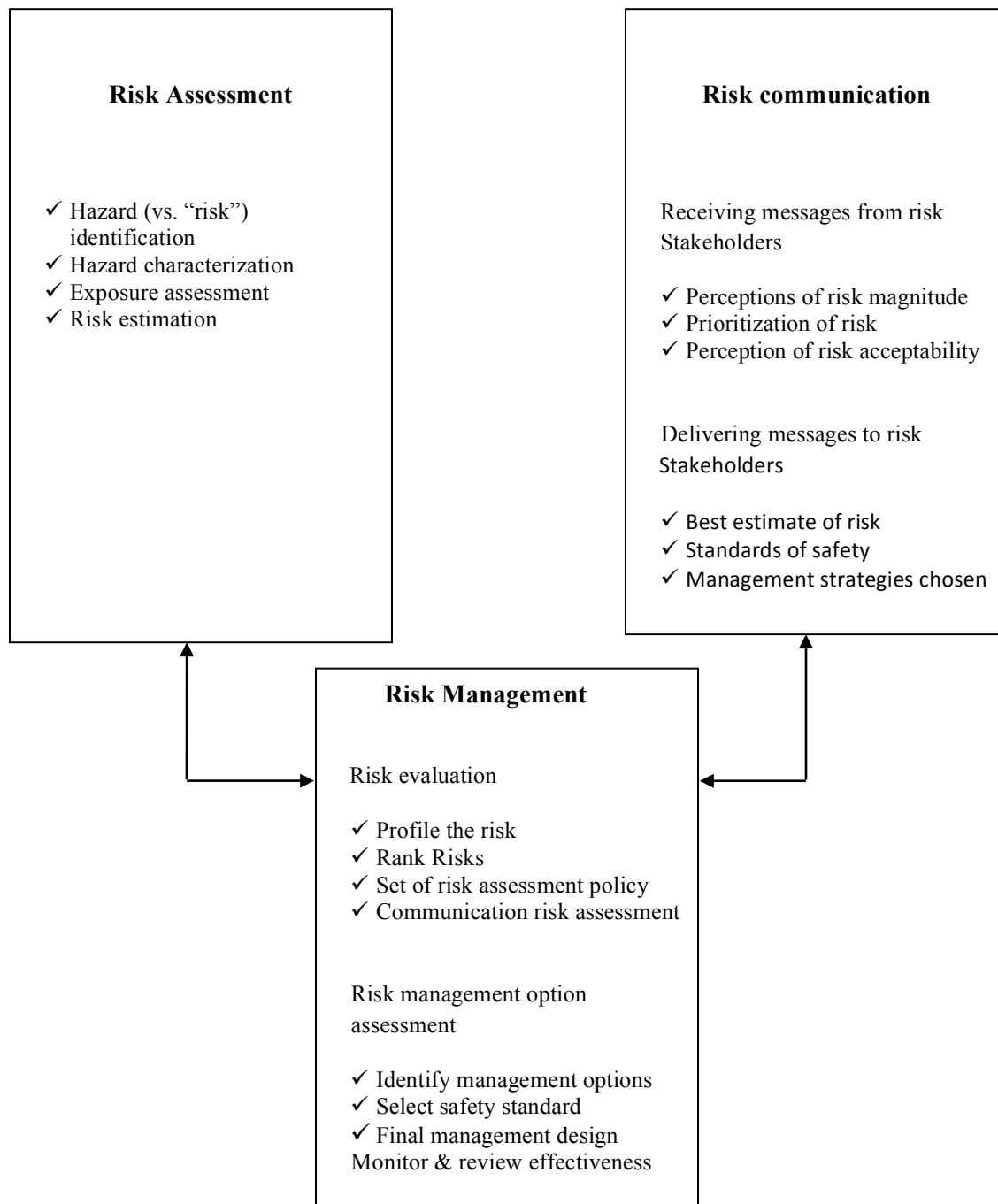


Figure 4.1. Different components of risk analysis (Brunk, 1998)

However, most environmental risk assessments are performed to answer a question or resolve an issue, such as: Is it safe for a proposed chemical plant to operate in this location or is it safe to dispose?

The Canadian Council of Ministers of the Environment (CCME) (1996/2007) has set forth guidelines for a three-tiered system that may be used to derive environmental quality criteria. The following components outlined by CCME are involved in the risk assessment process (CCME, 1996/2007):



Figure 4.2. Different components of risk assessment process (CCME, 1997)

As per Figure 4.2, the receptor is the person or population exposed to the contaminant at the exposure point. One of the important factors in determining exposure includes the characteristics of receptors. For most of the equations used to estimate the exposure, at least two terms (e.g. age, body weight and gender), attempt to define a specific receptor's characteristics or parameters. Some characteristics like body weight, volume of air inhaled per unit, amount of soil consumed inadvertently and time spent indoors and outdoors for human and ecological entities should be evaluated as a part of the environmental risk assessment process. The values for each of the receptors vary significantly and, for this reason, which receptors receive the greatest exposure from the contaminant needs to be defined.

Hazard, a measure of harm or the potential of the event to cause harm, is one of the components of the risk assessment process. Different types of hazards exist. Some are natural, while industrial or technological hazards are caused by human beings.

Exposure is one of the components of the analysis phase of a risk assessment. It is a measure of the amount that the likely recipient of a specific hazard absorbs. For any special hazard, the greater the exposure, the greater the risk of an adverse effect is on health. Exposure can be simply identified as the amount of the agent that is available to a human or animal. Exposure can occur through different pathways for humans, as illustrated in Figure 4.3. The absorption of chemicals is related to the route of exposure. Furthermore, the absorption of a chemical also is affected by its chemical and physical properties. In simple terms, chemicals that are soluble in fat can be absorbed more easily into the body.

These risk assessment processes are divided into different components according to different organizations such as Environmental Protection Agency (EPA) and CCME.

The EPA baseline risk assessment process includes data collection and evaluation, exposure assessment, toxicity assessment and risk characterization (USEPA, 1999), as can be seen in Figure 4.4.

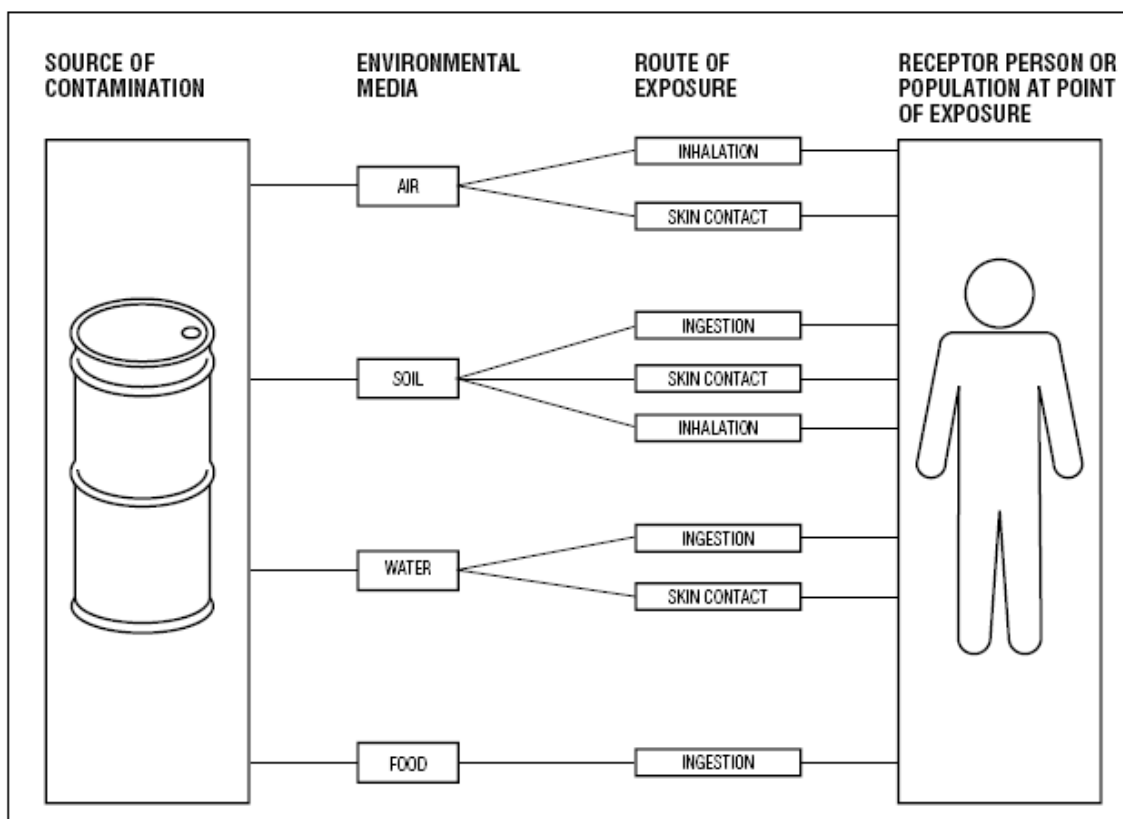


Figure 4.3. Major pathways of human exposure to environmental contaminants (Health Canada, 1995)

There are many different risk assessment approaches proposed by regulations agencies such as EPA and CCME. Most of these approaches are comprised of four steps, which are outlined below:

- ✓ Hazard identification and assessment
- ✓ Exposure assessment
- ✓ Dose-Response assessment
- ✓ Risk characterization

These four steps provide a better understanding of a system's environmental risk assessment. Thus, these steps are described in the following sections.

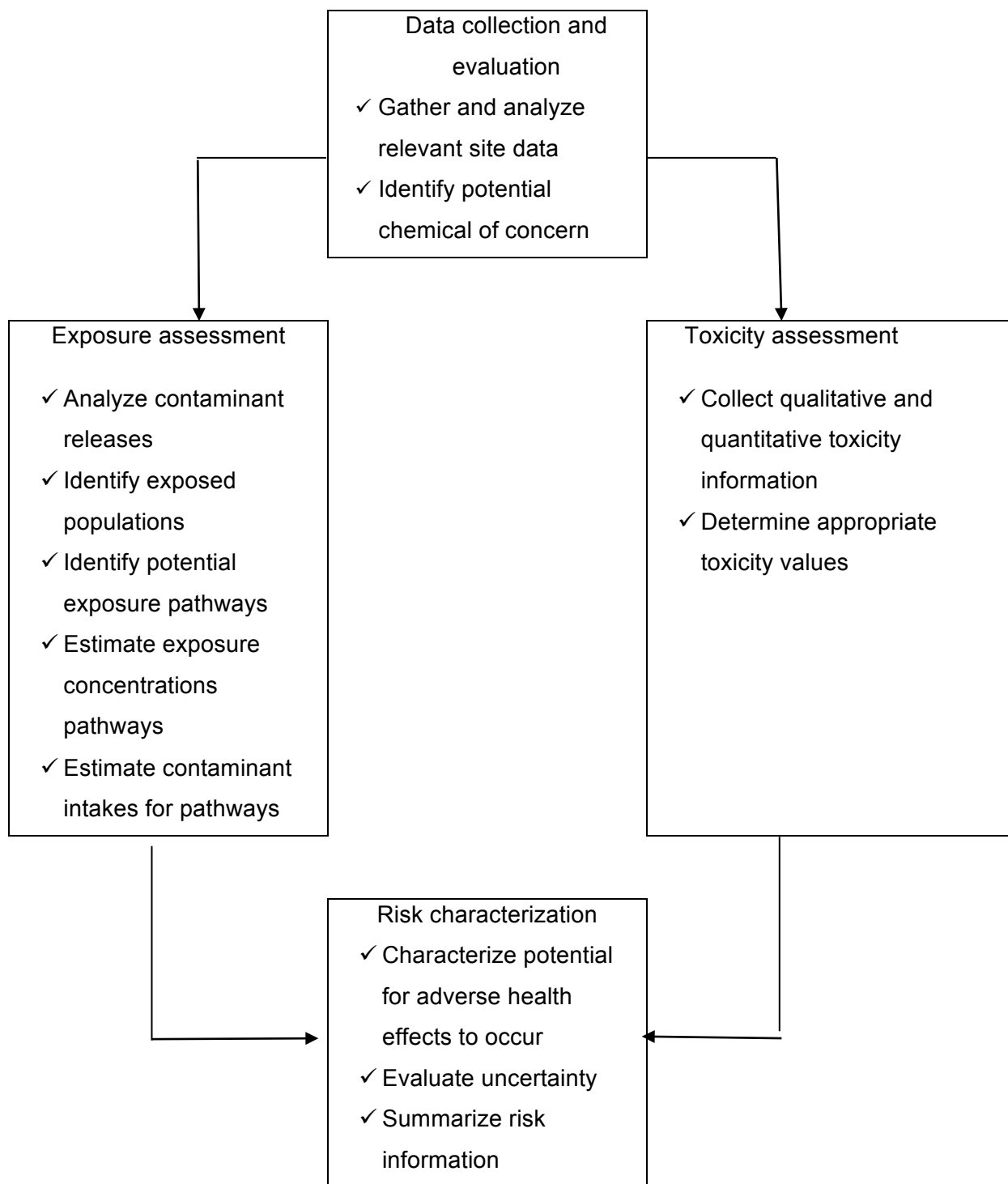


Figure 4.4. Different processes of risk assessment according to EPA (USEPA, 1999)

4.1.1. Hazard identification and assessment

The potential for chemicals to cause adverse effects on the lives of humans, plants and animals can be provided and understood by considering hazard assessment. Hazard identification is the first stage in hazard assessment (Phua et al., 2007). It includes gathering and evaluating toxicity data on the types of health impact or disease that may be produced by a chemical and the conditions under which the impact or the disease is produced. In order to identify the hazard, the data for all contaminants at a site should be examined and the data to stress the chemicals of concern should be consolidated. The following steps show the data needed in hazard identification stages (Khan, 2008):

- Site history
- Land use
- Contaminant levels in media
 - ✓ Air
 - ✓ Ground water
 - ✓ Surface water
 - ✓ Soils and sediments
- Environmental characteristics affecting chemical fate and transport
 - ✓ Geologic
 - ✓ Hydrologic
 - ✓ Atmospheric
 - ✓ Topographic
- Potentially affected population
- Potentially affected biota

Hazard assessment is most commonly used for analyzing the effects of chemicals on the natural environment. The definition of hazard is formulated by Klopffer (1994) as follows:

$$\text{Hazard} = \text{Exposure} * \text{Effect} \quad (4.1)$$

This shows that there is no hazard (bad effect) if there is no exposure. The following steps are involved in hazard assessment:

- 1) The contaminant data should be sorted by medium (e.g. ground water, soil, etc.) for both carcinogens and non-carcinogens.
- 2) The average and range of each chemical concentration observed at the site should be demonstrated.

- 3) The toxicity scores (TS) for each chemical in each medium due to carcinogens and non-carcinogens should be demonstrated as follows:

For non-carcinogens: Considering exposure duration, the toxicity score is estimated as follows:

$$TS = \frac{C_{Max}}{RFC} \quad (4.2)$$

RFC = Chronic reference concentration (an estimate of acceptable daily intake)

$$\text{For carcinogens: } TS = SF * C_{Max} \quad (4.3)$$

SF = Slope factor (slope factor here is considered for daily intake
(slope factor * day))

- 4) Ranking the compounds by toxicity scores for each exposure route
- 5) For each exposure route, selecting those chemicals that compose 99 percent of the total score.

4.1.2. Exposure assessment

There has been a significant increase in awareness of environmental issues in recent years and there is a great concern among the people over how their health is affected by environmental factors. Exposure assessment includes estimating the dose or concentration of the contaminant taken in by human and ecological receptors per unit of time. Characterization of the exposure setting, identification of exposure pathways and quantification of exposure are different steps in exposure assessment.

Using the exposure assessment, the following questions can be answered:

- 1) Who and what is exposed (e.g. people, aquatic ecosystems)?
- 2) How much exposure occurs?
- 3) How often and how long does the exposure occur and what is its frequency and duration?

Various plausible exposure pathways exist for every valued ecosystem component. Different pathways include direct contact, water ingestion, soil or sediment ingestion, and through the food chains. Indirect contact should be considered as well.

Using the fate and transport model, which is validated through field measurement, the information for input into an exposure model can be provided. Different steps for calculating exposures to chemicals present in the environment can be seen in Figure 4.5.

For calculating people's and ecological entities' exposure to environmental contaminants, several assumptions need to be considered.

The average values are generally used for:

- Body weight
- Amount of food and water consumed
- Amount of air breathed, and
- Number of times people and ecological entities are exposed to contaminants over their lifetime

The exposure pathway describes how the contaminants go into the environment from their source to humans or other living organisms.

Exposure pathways include the following steps:

- Source of contamination
- Environmental media
- Point of exposure
- Receptor person or population; and
- Route of exposure

It is noteworthy that the source of environmental contaminants varies from place to place. It can consist of exhaust from cars, wastewater released by factories and mills, waste disposal sites or closed factories or disposal sites. Furthermore, a number of natural sources can release various substances into the environment.

When the contaminants are released from their sources, they can travel over different environmental media to reach the points where human exposures can occur. For humans, the major environmental media are water, air, food and soil. Figure 4.6 demonstrates how contaminants are transported through the food chain and affect human health through exposure and food intake.

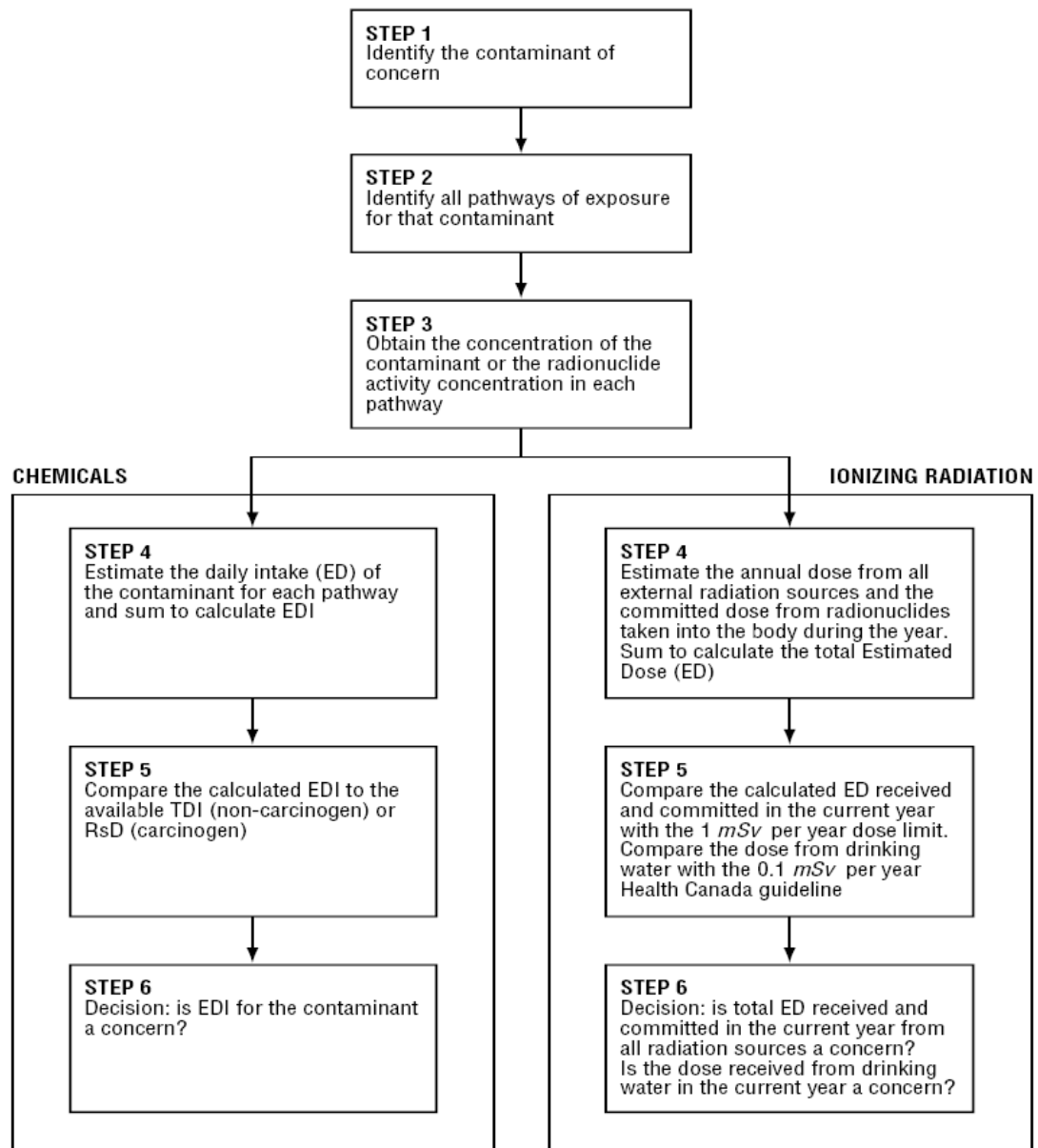


Figure 4.5. Different steps for calculating exposure to chemicals (Health Canada, 1995)

The point of exposure is where contact with the contaminants occurs. Different locations that people are exposed during the day and night (e.g. homes, workplaces, lakes, rivers or other bodies of water) can be the point of exposure.

The individual or population that is exposed to the contaminant at the point of exposure is the receptor. For example, people may be exposed to the contaminated air by going outside and breathing. Finally, the route of exposure is the way that the contaminant enters into the human and animal body. Ingestion, inhalation and skin contact are three general routes by which human and animals take the contaminant into their body.

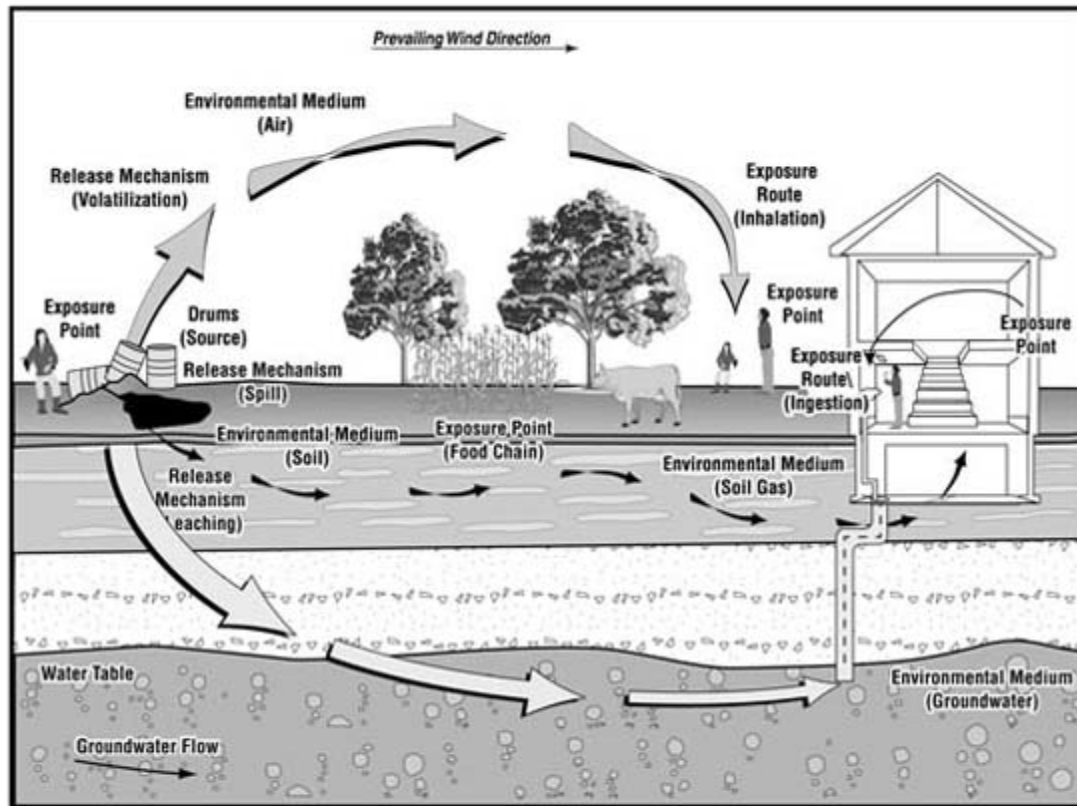


Figure 4.6. Exposure pathways schematic (ATSDR, n.d.)

After determining the different parts of exposure pathways, the exposure factor should be calculated in each pathway of exposure.

As mentioned above, inhalation of the contaminant is one of the pathways of exposure. The amount of a contaminant absorbed into the body by inhalation can be found by the following equation:

$$ED_a = \frac{C * IR * EF}{BW} \quad (4.4)$$

C = Concentration of contaminant in the air (mg/m³ of air)

The inhalation rate and average body weight for each person according to that person's sex and age can be seen in Table 2.6 and 2.7 (USEPA, 1997).

Table 4.1. Average body weight for each age group according to their sex (USEPA, 1997)

Model Age Group	Body Weight (kg)	
	Male	Female
0-17	34.3	33.0
18-44	78.2	64.3
45-64	79.9	68.0
65+	74.8	66.6

Table 4.2. EPA recommended inhalation values (USEPA, 1997)

Age Group (years)	Sex	Inhalation values (m ³ /day)
<1	Both	4.5
1-2	Both	6.8
3-5	Both	8.3
6-8	Both	10
9-11	Male	14
	Female	13
12-14	Male	15
	Female	12
15-18	Male	17
	Female	12
19-65+	Male	11.3
	Female	15.2

Moreover, the amount of a contaminant taken into the body per food is calculated for each individual food by the following equation:

(Food group 1) (Food group 2)

$$ED_f = \frac{CF * CR * EF}{BW} + \frac{CF * CR * EF}{BW} \quad (4.5)$$

4.1.3. Dose-Response assessment

Dose-Response assessment is the step of the risk assessment process that connects the likelihood and severity of damage on human health from exposures to different levels of risk agents. The quantitative relationship between the level of exposure and the intensity of the resulting adverse health effects is represented by graphs. This graph, which can be seen in Figure 2.14, shows the cumulative exposure or rate of exposure per unit of time.

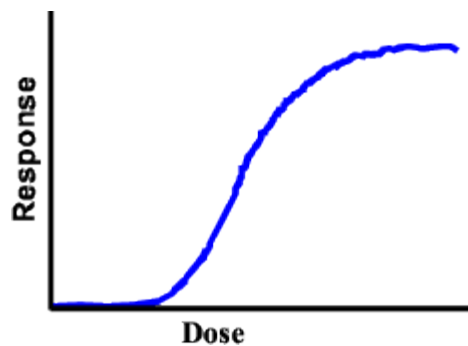


Figure 4.7. Dose-Response curve (USEPA, 1991)

The extrapolation of dose relationships from a specific population to another group or from animal studies to human beings should be conducted according to the following factors:

- ✓ Difference in physical dimensions like body weights
- ✓ Difference in intake
- ✓ Different life span
- ✓ Difference in the absorption rate of chemical, nature, routes.

Regression methods can be used for finding the dose and response relationship if enough data are available. Dose-Response models can be divided into three main categories. These categories are described in the following paragraphs.

Simple Dose-Response models: These models show the single measurement of dose (e.g. cumulative exposure) to a single measure health response (e.g. number of fatalities). These models are used to estimate the number of cases of cancer caused by exposure to low level radiation. For applications of this model, dose-response relationships are usually shown by curves with thresholds.

Tolerance distribution models: These models are based on the fact that each person in the population has an individual threshold tolerance associated with the specific risk agent. In these models, it is assumed that the probability that a particular individual will experience an adverse effect when exposed at the dose level d is the same as the probability for the tolerance level of the individual less than d . The log-probit model is the most commonly used tolerance models. It is popular because the result of toxicity tests often fit the shape assumed in the model. This model is usually used for determining the dose-response of the exposure to toxic gases and estimation of infections from disease caused by organisms.

Mechanistic models: These models usually show the biological processes that lead to an adverse effect as a series of events evolving over time. Although such models can become mathematically complex, they are usually based on very simple biological assumptions. Hit, multistage, and cellular proliferation models are the most well-known in this case (Fjeld, 2006). Mathematical equations of different dose-response models can be seen in Table 2.8.

Table 4.3. Mathematical equations of several dose-response models used in cancer risk assessment (Edler et al., 1998)

Model	Equations for the probability of response (Proportion of population affected at dose d)	Parameter constraints
Probit	$F(d) = \phi(a + b \ln d)$	$b > 0$
Logit	$F(d) = [1 - \exp(-(a + b \ln d))]^{-1}$	$b > 0$
Weibull	$F(d) = 1 - \exp(-bd^k)$	$b > 0, K > 0$
One hit	$P(d) = [1 - \exp(-bd)]$	$b > 0$
Multistage	$F(d) = [1 - \exp(-\sum_{i=0}^k a_i d^i)]$	$a_i \geq 0$

The standard procedure for assessing non-cancer risks related to hazardous components uses a No Observed Adverse Effect Level (NOAEL) approach. NOAEL is the point in which no-effect level is observed. By applying an uncertainty factor to this point, it may be then used to estimate a dose limit for humans. This limit is below a presumed threshold and shows the acceptable exposure level. For establishing a permissible exposure levels for humans for non-carcinogens, the NOAEL is used for finding the RFD (Reference Dose) as follows:

$$RFD = \frac{NOAEL}{UF} \quad (4.6)$$

UF is the uncertainty factor, which is assumed to be 10 when relevant research based information is missing.

In a new dose-response procedure, the benchmark dose method is used instead of NOAEL. In benchmark modeling, the bench mark (BM), which is the dose related to 10% response, is evaluated. The lower bond of 95% confidence interval for this BM is called LBM (Faustman, 1996).

To determine the best model that can fit the dose and response data, EPA develops the Benchmark Dose Software (BMDS) to facilitate the application of benchmark dose (BMD) methods to the EPA hazardous pollutant risk assessment. This software helps find the Bench Mark (BM) and Lower Bond of 95% of confidence interval (LBM) associated with different doses and responses. After finding BM and LBM, the RFD is calculated as follows:

$$RFD = \frac{BM, LBM}{UF} \quad (4.7)$$

A different approach is used for carcinogens which are generally assumed to have a non-threshold dose-response. A decision about these chemicals (carcinogens) must be made to determine “how large a risk of cancer can be accepted, in order to set acceptable intake levels” (Health Canada, 1995). Different acceptable levels of risk are used around the world. These levels vary between one extra cancer death per ten thousand people and one extra cancer death per million people exposed to the contaminants over their entire lifetime.

After establishing the acceptable level of risk, a dose that people can be exposed to on a daily basis over their entire lifetime that will not exceed the accepted level of risk of cancer can be calculated. As the acceptable dose is directly related to the decision about an acceptable level of risk, it is called Risk-specific Dose (RsD). Considering each carcinogen, which has its own slope factor, the RsD is calculated as follows (Health Canada, 1995):

$$RsD = \text{Acceptable level of risk} / \text{Slope factor} \quad (4.8)$$

4.1.4. Risk characterization

By integrating exposure assessment and toxicity assessment, which are discussed earlier, the probability of negative effects is understood. Risk characterization is carried out for individual chemicals and then summed for a mixture of chemicals (Considering that additivity is assumed). Next, the amount of

these chemicals can be compared with different guidelines on chemicals concentration. These guidelines suggest different criteria by considering different chemicals and ways of exposure.

Qualitative and quotient methods are suitable for risk characterization. The judgment will be relied on using qualitative methods, such as a ranking system that shows the level of risk in terms of high, moderate or low. If there is sufficient information available about the Expected Environmental Concentration (EEC) in the most important medium or media and where there are adequate studies available in the literature to determine the toxicological benchmark, the quotient method may be used. The quotient is calculated by “taking the ratio of the EEC and a BC (Benchmark Concentration) (CCME, 1996)”. If the quotient is less than 1, it shows that the risk is slight and little or no action is required. If the quotient is near 1, it shows uncertainty in the risk estimate and additional data is required. Finally, if the quotient is more than 1, it shows that the risk is greater and regulatory action may be indicated (CCME, 1996).

4.2. A developed risk-based methodology

A risk-based methodology based on the EPA framework integrated with the flare CFD modeling was developed to assess the effect of the flare gas emissions on human health downstream of the flare. The developed methodology can be found in Figure 4.9. Emissions predicted from the CFD model are passed to a stack dispersion model, which predicts species concentrations downstream of the flare (as a function of distance from flare). For concentrations at different distances, the hazard quotient method can be used to determine the effects of the flared gases. After adopting the species concentrations of the flared gases, and modeling the transport of contaminants at the downstream of the flare, the hazard quotient method can be used to consider the effects of the flared gases on human health.

By integrating exposure and toxicity assessment, the probability of negative effects is determined. Risk is calculated for individual chemicals and then summed for a mixture of chemicals (considering additive property of risk). The HQ is calculated by taking the ratio of exposure chemical concentration and TLV-TWA for each chemical of concern, as represented by Equation 4.9 (Abbassi et al., 2011).

$$HQ = \frac{\text{Exposure concentration}}{TLV-TWA} = \frac{\text{Concentration*time spend/BW}}{TLV-TWA/BW} \quad (4.9)$$

HQ is used to determine the distance from the flare which is safe for human exposure. Wherever the HQ is less than one, it demonstrates the inhaled species concentrations are less than the human tolerance level and there is no effect on the human health.

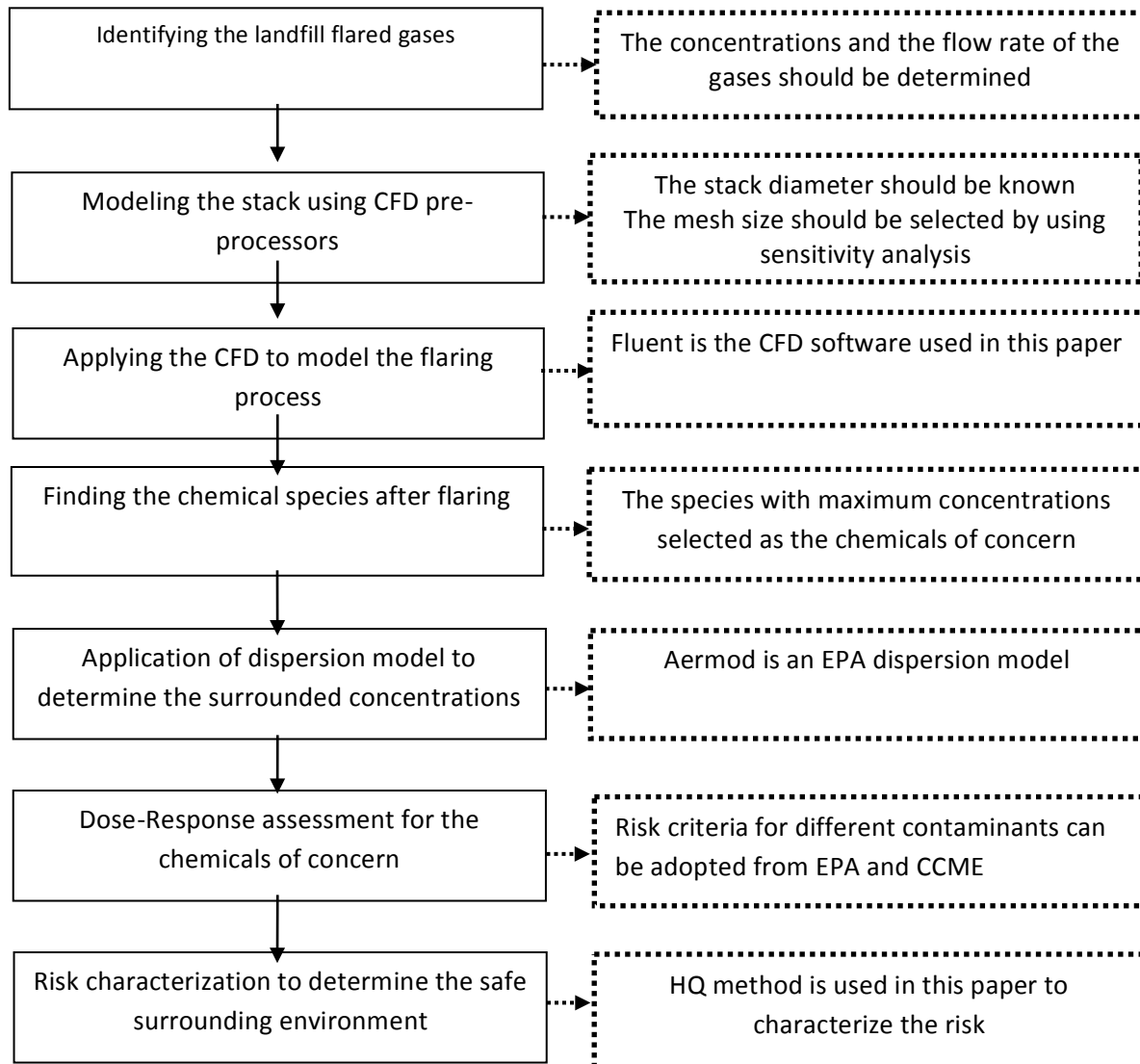


Figure 4.10. Risk-based methodology for evaluating a flare performance

4.3. A risk-based methodology: A case study

A risk-based methodology developed in section 4.2. has been applied to the case of the Kangiran flare. Although this case study is from oil and gas facilities, it has been adopted as it can provide us with the required information to illustrate the developed process. By having the required information of a landfill gas flare and surrounding environmental conditions, the same process developed in section 4.2 can be applied for managing the performance of a specific landfill flare.

4.3.1. Specification of a considered site

The Shahid Hashemi-Nejad (Khangiran) natural gas process facility is one of the most important gas processing facilities, located in northeastern Iran in an open inhabitable range land, semi arid and dusty with windblown sand. The feed gas is supplied from the Mozdouran gas fields. This gas process facility consists of 5 sour gas treating unit, 3 dehydration units, 3 sulfur recovery units, 2 distillation units, 2 stabilizer units and 14 additional units related to other services. The wind direction in the Khangiran vicinity is from northwest to southeast. This condition occurs in the Khangiran gas process facility for 90% of the year. For the remainder of the year, the wind direction changes, and the wind blows from southeast to northwest. Wind roses were used to give a succinct view of how wind speed and direction are typically distributed and to determine the direction of the prevailing wind in the vicinity of Khangiran. During 10% of the year, the wind direction is 160 degrees, which causes the wind to carry toxic gases to the personnel dormitory. This dormitory is located 1050 meters away from the flare stack and it is 200 meters in length. The release time was considered to be 1 h.

4.3.2. Risk Analysis

SO₂ is the toxic gas considered during the release time (1 h) in this study. SO₂ is a colorless gas which smells like burnt matches. It can be oxidized to sulfur trioxide, which in the presence of water vapor is readily transformed to sulfuric acid mist. SO₂ with acute exposure of 5 ppm may cause dryness of nose and throat and a miserable increase in resistance to bronchial air flow. SO₂ increasing up to 6 to 8 ppm causes a decrease in tidal respiration volume. Sneezing, cough & eye irritation occur at 10 ppm. SO₂ concentration of 20 ppm may cause Bronchospasm and 50 ppm causes extreme discomfort, but no injury in less than a 30 minute exposure. Finally, inhalation of 1000 ppm more than 10 minutes causes death (Thienes and Haley, 1972). The Concentration of SO₂ in this modeling scenario is 100.63 kmole/hr.

The dispersion of SO₂ in the studied area has been estimated by using AERMOD. The results of this modeling are summarized in Table 4.4. demonstrated that personnel dormitory is covered by a plume with a concentration of more than 5 ppm of SO₂ released from the flared gases.

Table 4.4. Concentrations of SO₂ in two different areas considered in this modeling scenario

Area	SO2 Concentration (ppm)	Number of Employees
1	2	200
2	5	220

Following the chemical concentrations estimated based on the considered model by applying AERMOD, the exposure factors considered in this modeling scenario (average) is shown in Table 4.5.

Table 4.5. Exposure factors in two different scenarios (USEPA, 1989)

Factors	Average
Inhalation rate (m ³ /hr)	0.72
Exposure time (hr/event)	12
Exposure frequently (events/yr)	269
Body weight (kg)	70

The reference concentration (RFC) is used to assess inhalation risks, where concentration refers to levels of contaminants in the air. The reference concentration of SO₂ is 0.078 mg/m³ and considered to calculate the final HQ.

Finally, by integrating exposure assessment and toxicity assessment, which are discussed previously, the probability of negative effects is assumed. The value of HQs for inhaling SO₂ in two different regions considered in this study can be seen in Table 4.6.

Table 4.6. Calculating hazard quotients in different area considered in this modeling

Area	SO ₂ Concentration (ppm)
1	0.68E02
2	1.71E02

As can be seen in Table 4.6, the value of HQs in both regions considered in this modeling are much higher than one. This illustrated that the employees inhaling air in both regions encounter a high level of risk. As a result, the amount of gases released in the studied area should be decreased. In this way, application of environmental risk assessment can provide an opportunity to see the efficiency of the treatment system, and to manage it in the required area. The methodology developed in section 4.2 by integrating the environmental risk assessment framework with CFD provides a key to manage the landfill flaring process to reach the optimum efficiency to comply with the regulatory guidelines.

We can apply this same methodology to our CFD model emissions. In the gas of the above gas plant, and any landfill, prior knowledge of emission dispersion would provide operators with information to better design ambient monitoring systems and better manage flare operations based on atmospheric conditions.

5.1. Conclusion

In this work we have developed a CFD model for use as a tool in landfill gas flaring. The costs associated with large scale testing of landfill flares and improper operation due to lack of predictive models could be reduced using the CFD model. We validated the model with published data and developed a method to scale up our model to accommodate the non-ideal mixing encountered in landfill flares. Finally we proposed methodology to integrate the CFD model with dispersion and risk models to evaluate environmental impact and which can be used as a tool in designing environmental monitoring networks. As the report indicates, the model is general but the input parameters will be a function of the specific landfill as the composition of the landfill gas is a function of waste, landfill age and season. The chemical reaction mechanism used must balance computational time and cost with emission predictions that reflect contaminants of concern and flame temperature (or combustion efficiency). By integrating the CFD and environmental risk assessment, we have a tool to manage the flaring which incorporates human and environmental health concerns.

5.2. Recommendations

Based on the investigations of the landfill gas flare composition and modeling of the flaring process using CFD, the authors are (contusing?) continuing the work:

1. Collection of data from local landfill flares and incinerators for input to our CFD model for a real case study
2. Modeling different processes such as steam injection and air injection, processes used to increase the efficiency of landfill gas flaring and validation of the results with real cases
3. Application of a methodology developed in this research to a landfill gas flare to create a field case study which identifies the carcinogenic and non-carcinogenic risks of flared gases.

Acknowledgements

The authors gratefully acknowledge the financial support provided by the Harris Centre of Memorial University under the Waste Management Applied Research Fund of 2010-2011.

References:

- Abbassi, R., Dadashzadeh, M., Khan, F. and Hawboldt, K. 2011. Risk-based prioritisation of indoor air pollution monitoring using computational fluid dynamics. *Indoor and Build Environment*, DOI: 10.1177/1420326X11428164
- Agency for Toxic Substances and Disease Registry (ATSDR): <http://www.atsdr.cdc.gov/>
- Alian, D. 1997. Landfill gas management in Canada. Proceedings of air and waste management association's annual meeting and exhibition, Quebec, Canada.
- Anonymous. 2010. Waste management opens first-ever private landfill gas to energy in south western Ontario. ON, Canada.
- Bilger, R.W., Starner, S.H., Kee, R.J. 1990. On reduced mechanisms for methane-air combustion in non-premixed flames. *Combustion and Flame*, 80: 135-149.
- Bondad, MGR., Arthur, J.R. and Subasinghe, R.P. 2008. Understanding and applying risk analysis in aquaculture. Rome, Italy: Food and Agriculture Organization of the United Nations.
- Brosseau, J., Heitz, M., 1994. Trace gas compounds from municipal landfill sanitary sites. *Atmos. Environ.* 28 (2), 285–293.
- Brunk, C. 1998. Risk management workshop.
<http://cmte.parl.gc.ca/Content/HOC/committee/362/envi/reports/rp1031697/envi01/15-ch8-e.html>
- Castiñeira, D., A. 2006a. Computational fluid dynamics simulation model for flare analysis and control. PhD thesis, Austin, Texas: The University of Texas at Austin.,.
- Castiñeira, D., and Edgar, T.F. 2006b. CFD for simulation of steam-assisted and air-assisted flare combustion systems. *Energy and Fuels*, 20(3): 1044-1056.
- Castiñeira, D., and Edgar, T.F. 2008a. CFD for simulation of crosswind on the efficiency of high momentum jet turbulent combustion flames. *Journal of Environmental Engineering*, 134(7): 561-571.
- Castiñeira, D., and Edgar, T.F. 2008b. Computational fluid dynamics for simulation of wind-tunnel experiments on flare combustion systems. *Energy and Fuels*, 22(3): 1698-1706.
- Canadian Council of Ministers of the Environment (CCME). 1996. A framework of ecological risk assessment: General guidance. The national contaminated sites remediation program, Winnipeg, Manitoba, Canada.
- Canadian Council of Ministers of the Environment (CCME). 2007. Canadian water quality guidelines for the protection of aquatic life.
- Covello, V.T., and Merkhofer, M.W. 1993. Risk assessment methods, approaches for assessing health and environmental risks. New York and London: Plenum Press, ISBN: 0-306-44382-1.
- Dincer, Faruk; Odabasi, Mustafa; Muezzinoglu, Aysen. *Journal of Chromatography A* vol. 1122 issue 1-2 July 28, 2006. p. 222-229

Edler, L., and Kopp-Schneider, A. 1998. Statistical models for low dose exposure. *Mutation Research*, 405: 227-236.

Eklund, B., Anderson, E.P., Walker, B.L. and Burrows, D.B. 1998. Characterization of landfill gas composition at the fresh kills municipal solid waste landfill. *Environmental Science and Technology*, 32: 2233-2237.

Environment Agency. 2002. Investigation of the composition, emissions and effects of trace components in landfill gas. R&D Project, P1-438.

Faustman, M.E. 1996. Review of Noncancer Risk assessment: Application of Benchmark Dose Methods. Department of environmental health, Seattle, WA: University of Washington.

Ferguson S. 2010. CD-adapco, http://www.kr.cd-adapco.com/press_events/Dynamics/27/flare.html#

Fjeld, R.A., Eisenberg, N.A, and Compton, K.L. 2006. Quantitative environmental risk analysis for human health. N.Y.: John Wiley & Sons, ISBN-13: 978-0-471-72243-4.

Fluent. 2012. User manuals 6.2. Fluent Inc.

Gottimukkala, B.C.V. 2008. CFD simulation of industrial flares with reduced mechanism and NOx dispersion from vehicular exhaust pipe. M.Sc. Thesis, Lamar University, Texas, USA.

Health Canada. 1995. Investigating human exposure to contaminants in the environment : A community handbook. Ottawa: Minister of National Health and Welfare, ISBN: 0-662-23543-6.

Karapidakis, E.S. and Tsava, A. 2010. Electric power production by biogas generation at Volos landfill in Greece. Department of natural resources and environment, Greece.

Khan, F.I. 2008. Risk assessment: Class handout. Memorial University of Newfoundland, St. John's, NL, Canada.

Kim, K.H., 2006. Emissions of reduced sulfur compounds (RSC) as a landfill gas (LFG): a comparative study of young and old landfill facilities. *Atmospheric Environment* 40: 6567–6578.

Klopffer, W. 1994. Environmental hazard Assessment of chemicals and products Part II: Persistence and degradability of organic chemicals. *Environmental science and pollution research*, 1(2): 108–116.

Lawal, S., Fairweather, M., Ingham, D., Ma, L., Pourkashanian, M. and Williams, A. 2010. Computational study of combustion in flares: structure and emission of a jet flame in turbulent cross-flow. GERG Academic Network Event, Brussels.

Mendiara, T. Alzueta, M.U. Millera, and Bilbao R., 2004, An Augmented Reduced Mechanism for Methane Combustion, *Energy and Fuels* 18(3).

Peters, N. and Kee, R.J. 1987. The Computation of stretched laminar methane-air diffusion flames using a reduced four-step mechanism. *Combustion and Flame*, 68(1): 17-29.

Phua, S.T.G., Davey, K.R., Daughtry, B.J. 2007. A new risk framework for predicting chemical residue(s)—Preliminary research for PCBs and PCDD/Fs in farmed Australian Southern Bluefin Tuna (*Thunnus maccoyii*). *Chemical engineering and processing*, 46(5): 491-496.

Stroscher, M. 1996. Investigations of flare gas emissions in Alberta. Final report to Environment Canada, Alberta Energy Utilities Board and the Canadian Association of Petroleum Producers, Calgary, Alberta, Canada.

Thienes, C., and Haley, T.J. 1972. Clinical Toxicology, 5th ed., Philadelphia: Lea and Febiger, , p. 198.

U.S. Environmental Protection Agency (USEPA). 1989. Exposure factors handbook, EPA/600/8-89/043.

U.S. Environmental Protection Agency (USEPA). 1991. Risk Assessment for Toxic Air Pollutants: A Citizen's Guide - EPA 450/3-90-024.

U.S. Environmental Protection Agency (USEPA). 1997. Exposure Factors Handbook. Office of Health and Environmental Assessment. Volumes 1 and 2. EPA/600/P-95/002Fa and EPA/600/P-95/002Fb.

U.S. Environmental Protection Agency (USEPA). 1998. Guidelines for ecological risk assessment, Risk assessment forum. EPA-630-R-98-002F. Washington, USA.

U.S. Environmental Protection Agency (USEPA). 1999. Office of solid waste, Media to receptor bio-concentration factors (BCFs).

Appendix 1

Reduced reaction mechanism considered in this research ($k=A*T^n \exp(-E_a/T)$) (REF????Z)

Reactions	A	n	T _a
1) $oh+o=h+o_2$	2.00E+14	-0.4	0.0
2) $o+h_2=oh+h$	5.06E+04	2.7	6290.0
3) $oh+h_2=h_2o+h$	2.10E+08	1.5	3450.0
4) $2oh=o+h_2o$	4.30E+03	2.7	-2486.0
5) $h+h+m=h_2+m$ h2o/0.0/	1.00E+18	-1.0	0.0
6) $h+h+h_2o=h_2+h_2o$	6.00E+19	-1.3	0.0
7) $h+o+m=oh+m$ h2o/5.0/	6.20E+16	-0.6	0.0
8) $h+oh+m=h_2o+m$ h2o/5.0/	1.60E+22	-2.0	0.0
9) $h+o_2+m=ho_2+m$ h2o/10.0/ n2/0.0/	2.10E+18	-1.0	0.0
10) $h+o_2+n_2=ho_2+n_2$	6.70E+19	-1.4	0.0
11) $h+ho_2=h_2+o_2$	4.30E+13	0.0	1411.0
12) $h+ho_2=2oh$	1.70E+14	0.0	874.0
13) $o+ho_2=o_2+oh$	3.30E+13	0.0	0.0
14) $co+o+m=co_2+m$ h2o/5.0/	6.20E+14	0.0	3000.0
15) $co+oh=co_2+h$	1.50E+07	1.3	-758.0
16) $ho_2+co=co_2+oh$	5.80E+13	0.0	22934.0
17) $ch_2o+oh=hco+h_2o$	3.40E+09	1.2	-447.0
18) $hco+m=h+co+m$ h2o/5.0/	1.90E+17	-1.0	17000.0
19) $hco+oh=h_2o+co$	1.00E+14	0.0	0.0
20) $hco+o_2=ho_2+co$	7.60E+12	0.0	400.0
21) $ch_3+h+m=ch_4+m$ h2o/8.57/ n2/1.43/	1.30E+16	-0.6	383.0
22) $ch_4+h=ch_3+h_2$	1.30E+04	3.0	8040.0
23) $ch_4+o=ch_3+oh$	1.00E+09	1.5	8600.0
24) $ch_4+oh=ch_3+h_2o$	1.60E+06	2.1	2460.0
25) $ch_4+o_2=ch_3+ho_2$	7.90E+13	0.0	56000.0
26) $ch_3+o=ch_2o+h$	8.40E+13	0.0	0.0
27) $ch_3+oh=ch_2+h_2o$	7.50E+06	2.0	5000.0
28) $ch_2(s)+h_2o=ch_3+oh$	3.00E+15	-0.6	0.0
29) $ch_2oh+h=ch_3+oh$	1.00E+14	0.0	0.0
30) $ch_3+oh+m=ch_3oh+m$ h2o/8.58/ n2/1.43/	6.30E+13	0.0	0.0
31) $ch_3+ho_2=ch_3o+oh$	8.00E+12	0.0	0.0

32) $\text{ch}_3+\text{o}_2=\text{ch}_3\text{o}+\text{o}$	2.90E+13	0.0	30480.0
33) $\text{ch}_3+\text{o}_2=\text{ch}_2\text{o}+\text{oh}$	1.90E+12	0.0	20315.0
34) $\text{ch}_3+\text{ch}_3+\text{m}=\text{c}_2\text{h}_6+\text{m}$	2.10E+16	-1.0	620.0
35) $\text{h}_2\text{o}/8.59/ \text{ n}_2/1.43/ \text{ h}_2/2.00/ \text{ co}/2.00/ \text{ co}_2/3.00/$			
36) $\text{ch}_3+\text{ch}_2\text{o}=\text{ch}_4+\text{hco}$	7.80E-08	6.1	1967.0
37) $\text{ch}_2+\text{o}_2=\text{co}+\text{h}_2\text{o}$	2.20E+22	-3.3	2867.0
38) $\text{ch}_2+\text{o}_2=\text{ch}_2\text{o}+\text{o}$	3.30E+21	-3.3	2867.0
39) $\text{ch}_2+\text{ch}_3=\text{c}_2\text{h}_4+\text{h}$	4.20E+13	0.0	0.0
40) $\text{ch}_2(\text{s})+\text{h}_2\text{o}=\text{ch}_2+\text{h}_2\text{o}$	3.00E+13	0.0	0.0
$\text{ch}_2(\text{s})+\text{o}_2=\text{co}+\text{oh}+\text{h}$	7.00E+13	0.0	0.0
41) $\text{ch}_3\text{oh}+\text{o}=\text{ch}_2\text{oh}+\text{oh}$	3.90E+05	2.5	3080.0
42) $\text{ch}_2\text{o}+\text{h}+\text{m}=\text{ch}_3\text{o}+\text{m}$	5.40E+11	0.5	2600.0
$\text{h}_2\text{o}/8.58/ \text{ n}_2/1.43/$			
43) $\text{h}+\text{ch}_2\text{o}+\text{m}=\text{ch}_2\text{oh}+\text{m}$	5.40E+11	0.5	3600.0
$\text{h}_2\text{o}/8.58/ \text{ n}_2/1.43/ \text{ h}_2/2.00/ \text{ co}/2.00/ \text{ co}_2/3.00/$			
44) $\text{ch}_2\text{oh}+\text{o}_2=\text{ch}_2\text{o}+\text{ho}_2$	7.20E+13	0.0	3577.0
45) $\text{c}_2\text{h}_6+\text{h}=\text{c}_2\text{h}_5+\text{h}_2$	5.40E+02	3.5	5210.0
46) $\text{c}_2\text{h}_6+\text{oh}=\text{c}_2\text{h}_5+\text{h}_2\text{o}$	7.20E+06	2.0	864.0
47) $\text{c}_2\text{h}_6+\text{ch}_3=\text{c}_2\text{h}_5+\text{ch}_4$	5.50E-01	4.0	8300.0
48) $\text{c}_2\text{h}_4+\text{h}+\text{m}=\text{c}_2\text{h}_5+\text{m}$	1.10E+12	0.5	1822.0
$\text{h}_2\text{o}/5.00/$			
49) $\text{c}_2\text{h}_5+\text{h}=\text{ch}_3+\text{ch}_3$	4.90E+12	0.3	0.0
50) $\text{c}_2\text{h}_5+\text{o}=\text{ch}_3\text{cho}+\text{h}$	5.30E+13	0.0	0.0
51) $\text{c}_2\text{h}_4+\text{m}=\text{c}_2\text{h}_2+\text{h}_2+\text{m}$	3.50E+16	0.0	71500.0
$\text{h}_2\text{o}/10.0/ \text{ n}_2/1.50/$			
52) $\text{c}_2\text{h}_4+\text{h}=\text{c}_2\text{h}_3+\text{h}_2$	5.40E+14	0.0	14900.0
53) $\text{c}_2\text{h}_4+\text{o}=\text{ch}_2\text{cho}+\text{h}$	4.70E+06	1.9	180.0
54) $\text{c}_2\text{h}_4+\text{o}=\text{ch}_3+\text{hco}$	8.10E+06	1.9	180.0
55) $\text{c}_2\text{h}_4+\text{oh}=\text{c}_2\text{h}_3+\text{h}_2\text{o}$	2.00E+13	0.0	5940.0
56) $\text{h}+\text{c}_2\text{h}_2+\text{m}=\text{c}_2\text{h}_3+\text{m}$	3.10E+11	0.6	2590.0
$\text{h}_2\text{o}/5.00/ \text{ h}_2/2.00/ \text{ co}/2.00/ \text{ co}_2/3.0/$			
57) $\text{c}_2\text{h}_3+\text{o}_2=\text{ch}_2\text{o}+\text{hco}$	1.10E+23	-3.3	3890.0
58) $\text{c}_2\text{h}_3+\text{o}_2=\text{ch}_2\text{cho}+\text{o}$	2.50E+15	-0.8	3135.0
59) $\text{c}_2\text{h}_3+\text{o}_2=\text{c}_2\text{h}_2+\text{ho}_2$	5.20E+15	-1.3	3310.0
60) $\text{c}_2\text{h}_2+\text{o}=\text{hcco}+\text{h}$	1.40E+07	2.0	1900.0
61) $\text{ch}_3\text{cho}+\text{oh}=\text{ch}_3\text{co}+\text{h}_2\text{o}$	2.30E+10	0.7	-1110.0
62) $\text{ch}_2\text{cho}+\text{h}=\text{ch}_3+\text{hco}$	1.00E+14	0.0	0.0
63) $\text{ch}_2\text{cho}+\text{h}=\text{ch}_3\text{co}+\text{h}$	3.00E+13	0.0	0.0
64) $\text{ch}_2\text{cho}+\text{oh}=\text{ch}_2\text{co}+\text{h}_2\text{o}$	2.00E+13	0.0	0.0
65) $\text{ch}_2\text{cho}+\text{o}_2=\text{ch}_2\text{o}+\text{co}+\text{oh}$	2.20E+11	0.0	1500.0
66) $\text{ch}_2\text{cho}+\text{ch}_3=\text{c}_2\text{h}_5\text{cho}$	5.00E+13	0.0	0.0
67) $\text{c}_2\text{h}_5+\text{hco}=\text{c}_2\text{h}_5\text{cho}$	1.80E+13	0.0	0.0
68) $\text{c}_2\text{h}_5\text{cho}+\text{h}=\text{c}_2\text{h}_5\text{co}+\text{h}_2$	8.00e+13	0.0	0.0
69) $\text{c}_2\text{h}_5\text{cho}+\text{oh}=\text{c}_2\text{h}_5\text{co}+\text{h}_2\text{o}$	1.2e+13	0.0	0.0
70) $\text{ch}_2\text{co}+\text{oh}=\text{hcco}+\text{h}_2\text{o}$	1.00E+07	2.0	3000.0
71) $\text{h}+\text{hcco}=\text{ch}_2+\text{co}$	1.00E+14	0.0	0.0
72) $\text{hcco}+\text{o}_2=\text{co}_2+\text{co}+\text{h}$	1.40E+07	1.7	1000.0
73) $\text{hcco}+\text{o}_2=\text{co}+\text{co}+\text{oh}$	2.90E+07	1.7	1000.0

Appendix 2

Reduced reaction mechanism including H₂S ($k=A \cdot T^n \exp(-E_a/T)$)

Reactions	A	n	E _a
1) H ₂ S+M = S+H ₂ +M	1.600E+24	-2.6100	44800.00
2) N ₂ /1.5/ SO ₂ /10/ H ₂ O/10/			
3) H ₂ S+H = SH+H ₂	1.200E+07	2.1000	350.00
4) H ₂ S+O = SH+OH	7.500E+07	1.7500	1460.00
5) H ₂ S+OH = SH+H ₂ O	2.700E+12	0.0000	0.00
6) H ₂ S+S = 2SH	8.300E+13	0.0000	3700.00
7) H ₂ S+S = HS ₂ +H	2.000E+13	0.0000	3723.84
8) S+H ₂ = SH+H	1.400E+14	0.0000	9700.00
9) SH+O = H+SO	1.000E+14	0.0000	0.00
10) SH+OH = S+H ₂ O	1.000E+13	0.0000	0.00
11) SH+HO ₂ = HSO+OH	1.000E+12	0.0000	0.00
12) SH+O ₂ = HSO+O	1.900E+13	0.0000	9000.00
13) S+OH = H+SO	4.000E+13	0.0000	0.00
14) S+O ₂ = SO+O	5.200E+06	1.8100	-600.00
15) 2SH = S ₂ +H ₂	1.000E+12	0.0000	0.00
16) SH+S = S ₂ +H	1.000E+13	0.0000	0.00
17) S ₂ +M = 2S+M	4.800E+13	0.0000	38800.00
18) S ₂ +H+M = HS ₂ +M	1.000E+16	0.0000	0.00
N ₂ /1.5/ SO ₂ /10/ H ₂ O/10/			
19) S ₂ +O = SO+S	1.000E+13	0.0000	0.00
20) HS ₂ +H = S ₂ +H ₂	1.200E+07	2.1000	352.42
21) HS ₂ +O = S ₂ +OH	7.500E+07	1.8000	1460.00
22) HS ₂ +OH = S ₂ +H ₂ O	2.700E+12	0.0000	0.00
23) HS ₂ +S = S ₂ +SH	8.300E+13	0.0000	3700.00
24) HS ₂ +H+M = H ₂ S ₂ +M	1.000E+16	0.0000	0.00
N ₂ /1.5/ SO ₂ /10/ H ₂ O/10/			
25) H ₂ S ₂ +H = HS ₂ +H ₂	1.200E+07	2.1000	360.00
26) H ₂ S ₂ +O = HS ₂ +OH	7.500E+07	1.8000	1460.00
27) H ₂ S ₂ +OH = HS ₂ +H ₂ O	2.700E+12	0.0000	0.00
28) H ₂ S ₂ +S = HS ₂ +SH	8.300E+13	0.0000	3700.00
29) SO ₃ +H = HOSO+O	2.500E+05	2.9200	25300.00
30) SO ₃ +O = SO ₂ +O ₂	2.000E+12	0.0000	10000.00
31) SO ₃ +SO = 2SO ₂	1.000E+12	0.0000	5000.00
32) SO+O(+M) = SO ₂ (+M)	3.200E+13	0.0000	0.00
N ₂ /1.5/ SO ₂ /10/ H ₂ O/10/			
LOW / 1.200E+21 -1.54 0.00 /			
TROE / 0.5500 1.0e-30 1e+30 /			
33) SO ₂ +O(+M) = SO ₃ (+M)	9.200E+10	0.0000	1200.00
LOW / 2.400E+28 -4.00 2640.00 /			

34) SO ₂ +OH(+M) = HOSO ₂ (+M)	5.7306E+12	-0.2700	0.00
LOW / 1.688E+27 -4.09 0.00 /			
TROE / 0.47 1e-30 1e30 /			
35) SO ₂ +OH = HOSO+O	3.900E+08	1.8900	38200.00
36) SO ₂ +OH = SO ₃ +H	4.900E+02	2.6900	12000.00
37) SO ₂ +CO = SO+CO ₂	2.700E+12	0.0000	24300.00
38) SO+M = S+O+M	4.000E+14	0.0000	54000.00
N ₂ /1.5/ SO ₂ /10/ H ₂ O/10/			
39) SO+H+M = HSO+M	5.000E+15	0.0000	0.00
N ₂ /1.5/ SO ₂ /10/ H ₂ O/10/			
40) HOSO(+M) = SO+OH(+M)	9.940E+21	-2.5400	38190.00
LOW / 1.156E+46 -9.02 26647.00 /			
TROE / 9.5000E-01 2.9890E+03 1.1000E+00 /			
41) SO+OH = SO ₂ +H 1.077E+17 -1.35 0			
42) SO+O ₂ = SO ₂ +O	7.600E+03	2.3700	1500.00
43) 2SO = SO ₂ +S	2.000E+12	0.0000	2000.00
44) HSO+H = HSOH	2.500E+20	-3.1400	460.00
45) HSO+H = SH+OH	4.900E+19	-1.8600	785.00
46) HSO+H = S+H ₂ O	1.600E+09	1.3700	-170.00
47) HSO+H = H ₂ SO	1.800E+17	-2.4700	25.00
48) HSO+H = H ₂ S+O	1.100E+06	1.0300	5230.00
49) HSO+H = SO+H ₂	1.000E+13	0.0000	0.00
50) HSO+O+M = HSO ₂ +M	1.100E+19	-1.7300	-25.00
51) HSO+O = SO ₂ +H	4.500E+14	-0.4000	0.00
52) HSO+O+M = HOSO+M	6.900E+19	-1.6100	800.00
53) HSO+O = O+HOS	4.800E+08	1.0200	2700.00
54) HSO+O = OH+SO	1.400E+13	0.1500	150.00
55) HSO+OH = HOSHO	5.200E+28	-5.4400	1600.00
56) HSO+OH = HOSO+H	5.300E+07	1.5700	1900.00
57) HSO+OH = SO+H ₂ O	1.700E+09	1.0300	235.00
58) HSO+O ₂ = SO ₂ +OH	1.000E+12	0.0000	5000.00
59) HSOH = SH+OH	2.800E+39	-8.7500	37800.00
60) HSOH = S+H ₂ O	5.800E+29	-5.6000	27400.00
61) HSOH = H ₂ S+O	9.800E+16	-3.4000	43500.00
62) H ₂ SO = H ₂ S+O	4.900E+28	-6.6600	36000.00
63) H+SO ₂ (+M) = HOSO(+M)	3.119E+08	1.6100	3606.00
LOW / 2.662E+38 -6.43 5577.00 /			
TROE / 8.2000E-01 1.3088E+05 2.6600E+02 /			
64) HOSO+M = O+HOS+M	2.500E+30	-4.8000	60000.00
65) HOSO+H = SO ₂ +H ₂	3.000E+13	0.0000	0.00
66) HOSO+H = SO+H ₂ O	6.300E-10	6.2900	-960.00
67) HOSO+OH = SO ₂ +H ₂ O	1.000E+12	0.0000	0.00
68) HOSO+O ₂ = HO ₂ +SO ₂	1.000E+12	0.0000	500.00
69) HSO ₂ +H = SO ₂ +H ₂	3.000E+13	0.0000	0.00
70) HSO ₂ +OH = SO ₂ +H ₂ O	1.000E+13	0.0000	0.00
71) HSO ₂ +O ₂ = HO ₂ +SO ₂	1.000E+13	0.0000	0.00
72) H+SO ₂ (+M) = HSO ₂ (+M)	1.060E+09	1.4800	594.60
LOW / 1.251E+31 -5.17 1563.00 /			

TROE /	4.5000E-01	9.3550E+02	4.2700E+01	/
73) HOSO2 = HOSO+O	5.400E+18	-2.3400	53500.00	
74) HOSO2 = SO3+H	1.400E+18	-2.9100	27600.00	
75) HOSO2+H = SO2+H2O	1.000E+12	0.0000	0.00	
76) HOSO2+O = SO3+OH	5.000E+12	0.0000	0.00	
77) HOSO2+OH = SO3+H2O	1.000E+12	0.0000	0.00	
78) HOSO2+O2 = HO2+SO3	7.800E+11	0.0000	330.00	
79) HOSHO = HOSO+H	6.400E+30	-5.8900	37100.00	
80) HOSHO = SO+H2O	1.200E+24	-3.5900	30000.00	
81) HOSHO+H = HOSO+H2	1.000E+12	0.0000	0.00	
82) HOSHO+O = HOSO+OH	5.000E+12	0.0000	0.00	
83) HOSHO+OH = HOSO+H2O	1.000E+12	0.0000	0.00	
84) C+SO2 = CO+SO	4.156E+13	0.00	0.00	
85) HOSO2+H = SO3+H2	1.0E+12	0.00	0.00	
86) S+CH4 = SH+CH3	6.0e14	0.00	12078.42	
87) H2S+CH3 = CH4+SH	1.8E11	0.00	1177.53	
88) SH+O = S+OH	6.3e11	0.5	4030.55	
89) C+H2S = CH+SH	1.2e14	0.00	4450.32	
90) O+COS = CO+SO	1.93e13	0.00	2328.6	
91) O+CS = CO+S	1.626E+14	0.00	760.16	
92) COS+M = CO+S+M	1.43E14	0.00	30700.02	
93) O+COS = CO2+S	5E+13	0.00	5530.43	
94) SH+O2 = SO+OH	1.0e12	0.00	5032.48	
95) CH+SO = CO+SH	1.0e13	0.00	0.00	
96) SO3+S = SO+SO2	5.120E+11	0.00	0.00	
97) SH+NO = SN+OH	1.0E+13	0.00	8900.65	
98) S+NO = SN+O	1e12	0.5	17500.6	
99) SH+NH = SN+H2	1.0E+14	0.00	0.00	
100) N+SO = NO+S	6.31E+11	0.50	1010.34	
101) N+SH = SN+H	6.31E+11	0.50	4030.55	
102) SN+NO = N2+SO	1.807e10	0.00	00.0	
103) SN+O2 = SO+NO	3e8	0.00	00.0	
104) SN+NO2=S+NO+NO	4.068e15	-0.9805	00.0	
105) N+SN = N2+S	6.3e11	0.50	00.0	
106) SO2+NO2 = NO+SO3	4.25e-19	8.90	3797.21	
107) SO+NO2 = SO2+NO	8.432E+12	0.00	0.00	
108) SN+O = SO+N	6.31E+11	0.50	4030.55	
109) S+NH = SH+N	1.0E+13	0.00	0.00	
110) NH+SO = NO+SH	3.012e13	0.00	0.00	
111) HSO+NO2 = HOSO+NO	5.8E12	0.00	0.00	
112) SO3+H2O = H2SO4	7.230E+08	0.00	0.00	



THE LESLIE HARRIS CENTRE OF REGIONAL POLICY AND DEVELOPMENT

1st Floor Spencer Hall, St. John's, NL Canada A1C 5S7

Tel: 709 864 6170 Fax: 709 864 3734 www.mun.ca/harriscentre

THE HARRIS CENTRE Memorial University

